Available online at www.sciencedirect.com
SCIENCE DIRECT®
ELSEVIER
Journal of Constructional Steel Research 59 (2003) 1477–1497
JOURNAL OF CONSTRUCTIONAL STEEL RESEARCH
www.elsevier.com/locate/jcsr

Seismic design of steel structures with buckling-restrained knee braces

Jinkoo Kim *, Youngill Seo

Department of Architectural Engineering, Sungkyunkwan University, Chunchun-Dong, Jangan-Gu, 440-746 Suwon, South Korea

Received 26 January 2003; received in revised form 28 June 2003; accepted 1 July 2003

Abstract

Analytical models and a performance-based seismic design procedure were developed for a structure with buckling-restrained knee-braces. The hinge-connected main structural members, such as beams and columns, were designed only for gravity loads, and the knee-braces were designed to resist all the lateral seismic load. The cross-sectional size of knee-braces was estimated using the equivalent damping required to be supplied to meet a given performance objective. Parametric study was performed with design variables such as slope and yield stress of the braces. According to the time-history analysis results of a five-story structure with buckling-restrained knee-braces, the maximum displacement of the model structure turned out to correspond well with the desired target displacement after it is retrofitted by knee braces following the proposed procedure.

Keywords: Buckling-restrained knee braces; Capacity spectrum method; Performance based seismic design

1. Introduction

The conventional philosophy of seismic design depends on inelastic deformation of structural members for dissipation of input earthquake energy. Therefore the structures designed following the procedure are subjected to damages in structural members after being shaken by a design-level earthquake. Significant expense will be required to repair or replace the damaged structural parts.

* Corresponding author. Tel.: +82-331-290-7583; fax: +82-31-290-7570.
E-mail address: jinkoo@skku.ac.kr (J. Kim).

0143-974X/$ - see front matter © 2003 Elsevier Ltd. All rights reserved.
doi:10.1016/S0143-974X(03)00100-7

The damage in main structural members induced by earthquake ground motion can be prevented by connecting beams and columns with hinges and designing them to resist only gravity load, and employing lateral-load resisting members to withstand all the lateral seismic load. In this case most of the energy dissipation and structural damages caused by an earthquake will be concentrated on the lateral-load resisting members and thus the main members will remain elastic. After earthquake the damaged lateral-load resisting members can be replaced with ease and at reasonable cost.

Steel braces are generally used as an economic means of providing lateral stiffness to a steel structure. However, the energy dissipation capacity of a steel braced-structure subjected to earthquake loads is highly limited due to the buckling of the braces, which is the main reason for most seismic design provisions to regulate lower response modification factor to a braced frame than to a moment frame. Recently it has been shown that the energy dissipation or damage prevention capacity of a steel framed structure can be greatly enhanced by employing buckling-restrained braces. The buckling-restrained braces usually consist of a steel core undergoing significant inelastic deformation when subjected to strong earthquake loads and a casing for restraining global and local buckling of the core element. According to previous research [1], a buckling-restrained brace exhibits stable hysteretic behavior with high energy dissipation capacity. As energy dissipation in braced frames mainly relies on the inelastic deformation of diagonal braces, the use of buckling-restrained braces greatly increases the energy dissipation capacity of the system and decreases the demand for inelastic deformation of the other structural members.

Even with the structural efficiency and cost effectiveness, a braced frame is not always favored by architects and building owners because the diagonal braces obstruct the flow planning and block the interior view. These shortcomings can be overcome, with some sacrifice in efficiency, by employing knee braces instead of diagonal braces. Recently Suita et al. [2] carried out experiments on beam-column joints with buckling-restrained knee braces (BRKB), and observed that they had stable energy-dissipation capacity.

In this study a performance-based seismic design procedure for a structure with BRKB is developed. Parametric study is performed to find out proper slope of the knee braces. The hinge-connected beams and columns are designed for gravity loads, and the knee braces are designed to resist the code-defined seismic load. The seismic performance of the code-designed knee-braced structure is evaluated using the capacity spectrum method (CSM). Then the required amount of equivalent damping to satisfy given performance acceptance criteria is obtained in the framework of the performance-based seismic design concept. From the computed equivalent damping the size of the BRKB in each story required to be supplemented to the structure to meet the given performance objective is determined. The proposed method is applied to a five-story structure, and the maximum displacements obtained from time–history analysis are compared to the target displacement to check the accuracy of the proposed method.

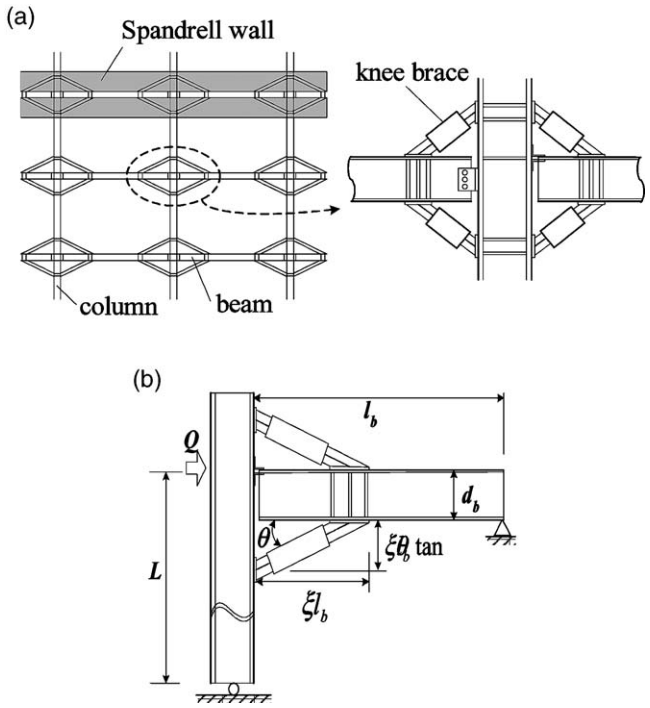

Fig. 1. Structure with buckling-restrained knee braces. (a) Side view of a structure with knee braces. (b) Analysis model.

2. Analytical models

Knee braces can be installed above and/or below the beams. Fig. 1(a) shows the beam-column connections with knee-braces placed both above and below the floor beams. The braces above the beams can be placed inside of curtain walls or partition walls, and those below the beams can be hidden above the ceiling. The lateral force-displacement relationship of a beam–column–brace unit is derived based on the system shown in Fig. 1(b). As the beam and column are connected by a hinge, the lateral load is mostly resisted by the braces. The beams and columns are generally stiffer than the knee braces, and are expected to remain elastic even after the braces yield.

The system shown in Fig. 1(b) can be divided into two types depending on the location of the hinge in the beam–column joint. The systems with the hinge located at the top flange of the beam and at the mid-height of the beam web are named as Type-T and Type-M, respectively. It is assumed in the derivation of the load–displacement relationship of the systems that the beam and the column are rigid, and that the brace shows elastic-perfectly plastic behavior.

Fig. 2(a) shows the deformed shape of the Type-T model. As lateral load increases, the lower brace which is located farther from the center of rotation yields prior

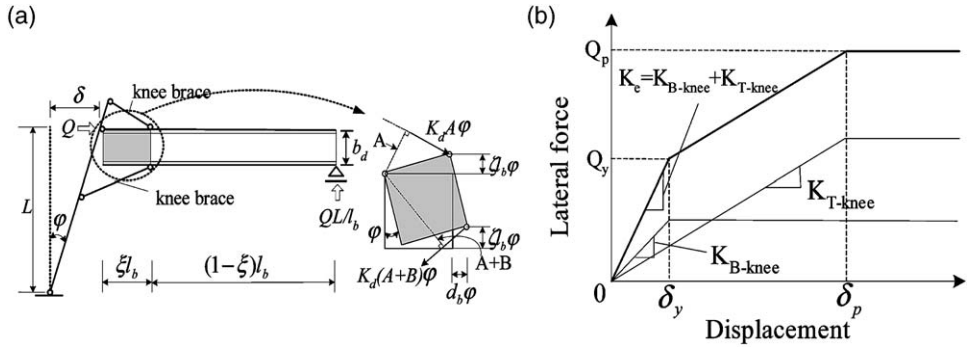

Fig. 2. Analysis model for Type-T system. (a) Analysis model. (b) Force–displacement relationship.

to the upper brace. This was observed in the experiments of Suita et al. [2]. Therefore the lateral load–displacement relationship of Type-T model can be divided into three different stiffness regions as described in Fig. 2(b):

1. the initial elastic stiffness which is the combination of the stiffness of both the upper and the lower braces;
2. the stiffness of the upper brace after the lower brace yields; and
3. zero stiffness after the upper brace yields.

The first two regions of stiffness can be obtained as follows:

$$K_e = K_B + K_T = \frac{K_d(A+B)^2}{L^2} + \frac{K_d A^2}{L^2}$$

$$= \frac{K_d(2A^2+2AB+B)^2}{L^2} \quad (0<\delta<\delta_y) K_e = K_T \quad (\delta_y<\delta<\delta_p), \tag{1}$$

where $A=\xi l_b \sin\theta$ and $B=d_b\cos\theta$; and $K_d = A_b E\cos\theta/\xi l_b$ is the axial stiffness of the brace, A_b is the cross-sectional area of the knee brace, l_b is the half the beam length, d_b is the depth of the beam, θ is the angle between the beam and the brace, ξ is the ratio of the horizontal projection of the brace and the half beam length, L is the height of the column, Q is the lateral load, δ is the lateral displacement, and δ_y is the lateral displacement at yield of the lower brace. The lateral load at the first yield of the lower brace is obtained as follows:

$$Q_y = \frac{N_y(A+B)+\phi K_d A^2}{L}, \tag{2a}$$

where N_y is the yield force of the knee brace. The lateral load at the yield of the upper brace is

$$Q_p = \frac{N_y(2A+B)}{L}. \tag{2b}$$

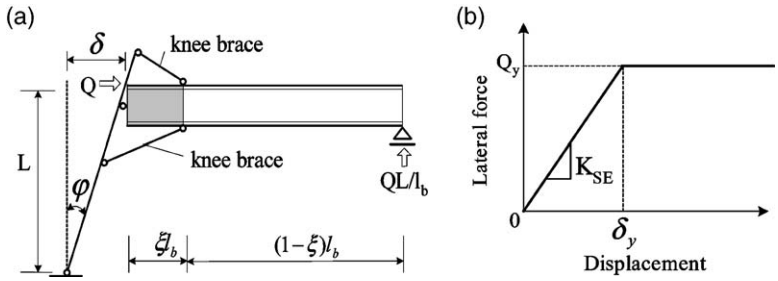

Fig. 3. Analysis model for Type-M system. (a) Analysis model. (b) Force–displacement relationship.

The lateral load–displacement relationship of the Type-M system, shown in Fig. 3(a), can be similarly obtained. If the cross-sectional areas of the upper and the lower braces are the same, the yielding of the braces will occur simultaneously. Therefore the load–displacement relationship is characterized by a bi-linear curve as shown in Fig. 3(b). The stiffness and the lateral load at yield can be obtained as follows:

$$K_e = \frac{Q}{\delta} = \frac{K_d(2A+B)^2}{2L^2} \tag{3}$$

$$Q_y = \frac{2N_y(A+B)}{L}. \tag{4}$$

Fig. 4(a) describes a beam–column system with a knee brace located only below the beam (named as Type-B), which is the same with the Type-T system without the upper brace. The load–displacement relationship can also be expressed by a bi-linear curve as shown in Fig. 3(b). The stiffness and the lateral load at yield can be obtained as follows:

$$K_{SE} = \frac{Q}{\delta} = \frac{K_d(A+B)^2}{L^2} \tag{5}$$

$$Q_y = \frac{N_y(A+B)}{L}. \tag{6}$$

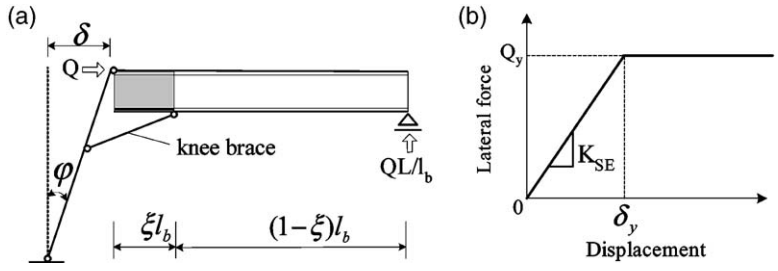

Fig. 4. Analysis model for Type-B system. (a) Analysis model. (b) Force–displacement relationship.

The load–displacement relationship is also characterized by a bi-linear curve as shown in Fig. 4(b).

The seismic design concept of the proposed structure system requires that the knee braces should yield first before the other structural members do. Therefore the bending moment acting on the beam-brace joint should be less than the yield moment of the beam, which requires that the cross-sectional area of knee braces should be limited to the following value:

$$A_b < \frac{\sigma_{fy} Z_f}{\sigma_{by} \sin\theta (1-\xi)\xi l_b}, \tag{7}$$

where σ_{fy} and Z_{fy} are the yield stress and the section modulus of the beam flange, respectively, and σ_{by} is the yield stress of the brace.

3. Performance-based design procedure

In this section a performance-based seismic design procedure for a structure with BRKBs is presented. The seismic performance of a structure is evaluated first by the CSM [4,5]. If the performance is not satisfactory, then the amount of equivalent damping required to meet the given performance objective is computed. The proper sizes of knee braces are determined from the required equivalent damping.

3.1. Seismic story force for pushover analysis

The relationship between the base shear and the top story displacement, which is generally called the pushover curve or capacity curve, is obtained by gradually increasing the lateral seismic story forces appropriately distributed over the stories. In this study the seismic story forces are applied in proportion to the product of the story mass and the fundamental mode shape coefficients of the structure:

$$F_i = \frac{m_i \phi_{i1}}{\sum_{i=1}^{N} m_i \phi_{i1}} V \tag{8}$$

where F_i and m_i are the seismic story force and the mass of the ith floor, respectively, ϕ_{i1} is the ith component of the mode shape vector for the fundamental mode, V is the base shear, and N is the number of floors.

3.2. Conversion to ADRS format

Application of the capacity spectrum technique requires that both the demand spectra and structural capacity curve be plotted in the spectral acceleration versus spectral displacement domain, which is known as acceleration–displacement response spectra (ADRS). To convert a response spectrum from the standard pseudo-acceleration S_a versus natural period T format to ADRS format, it is

necessary to determine the value of S_d for each point on the curve, S_a and T. This can be done using the equation

$$S_d = \left(\frac{T^2}{4\pi^2}\right) S_a g. \tag{9}$$

In order to develop the capacity spectrum from the capacity curve, it is necessary to do a point by point conversion to the first mode spectral coordinates. Any point of base-shear V and roof displacement Δ_R on the capacity curve is converted to the corresponding point S_a and S_d on the capacity spectrum using the equations:

$$\begin{aligned} S_a &= \frac{V}{M_1^*} \\ S_d &= \frac{\Delta_R}{\Gamma_1 \phi_{R1}}, \end{aligned} \tag{10}$$

where Γ_1 is the modal participation factor for the first natural mode of vibration and ϕ_{R1} is the roof level amplitude of the first mode. The mathematical expressions for the modal mass coefficient M_1^* is as follows:

$$M_1^* = \frac{\left(\sum_{j=1}^{N} m_j \phi_{j1}\right)^2}{\sum_{j=1}^{N} m_j \phi_{j1}^2}. \tag{11}$$

3.3. Estimation of effective period

A bilinear representation of the capacity spectrum, as described in Fig. 2, is needed to estimate the effective damping and appropriate reduction of spectral demand. ATC-40 recommends that the area under the original capacity curve and the equivalent bilinear curve be equal so that the energy associated with each curve is the same. When the bilinear system undergoes inelastic action at displacement S_{dp} with corresponding acceleration equal to S_{ap}, the effective period, T_{eff}, is determined from the secant (or effective) stiffness at maximum displacement [5]

$$T_{eff} = 2\pi \sqrt{\frac{S_{dp}}{S_{ap}}}. \tag{12}$$

3.4. Supplemental knee braces required to satisfy the given performance objective

In this section the proper size of BRKB needed to be supplemented for the structure to satisfy the given performance objective is evaluated. The total effective damping of a structure ζ_{eff} can be obtained as follows:

$$\zeta_{eff} = \zeta_s + \zeta_i, \tag{13}$$

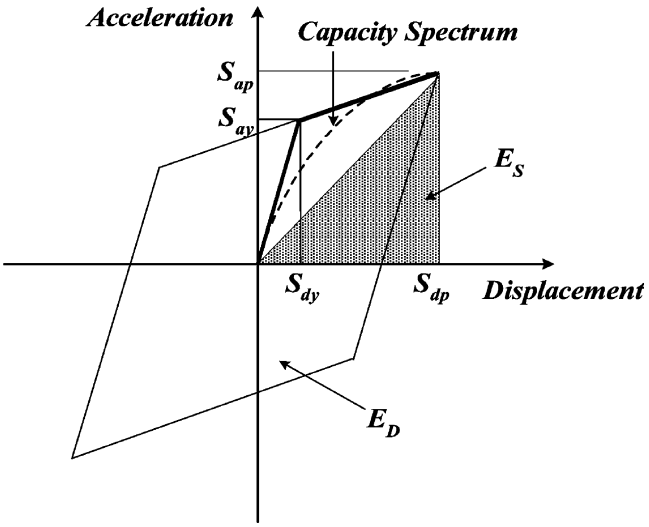

Fig. 5. Computation of equivalent damping.

where ζ_s is the hysteretic damping ratio contributed from the original structure obtained from Fig. 5 as follows

$$\zeta_s = \frac{1}{4\pi}\frac{E_D}{E_S} = \frac{2(S_{ay}S_{dp} - S_{dy}S_{ap})}{\pi S_{ap}S_{dp}}, \tag{14}$$

where E_D is the dissipated energy through hysteretic behavior of the structure, and E_S is the stored energy as described in Fig. 5. And ζ_i is the inherent viscous damping of the structure, for which 5% of the critical damping is generally assumed.

When the performance point exceeds the desired target point, the response can be reduced to the target by adding additional BRKB, which provides both stiffness and equivalent damping. The required amount of effective damping can be obtained on the ADRS format as shown in Fig. 6. The required overall effective damping of the system at the target displacement, ζ_{eff}, corresponds to the damping ratio of the demand spectrum that intersects the capacity curve at the target displacement on the ADRS. With the required overall effective damping at hand, the supplemental damping required to meet the performance point, ζ_{add}, can be obtained as follows:

$$\zeta_{add} = \zeta_{eff} - \zeta_s - \zeta_i. \tag{15}$$

The hysteretic damping contributed from the original structure is obtained from the capacity curve at the performance point. As the beams and columns remain elastic, the equivalent damping is provided by the inelastic deformation of the BRKB placed in the original structure.

Once the amount of damping required to be supplemented is obtained, the next step is to determine the size of the supplemental braces that can realize the

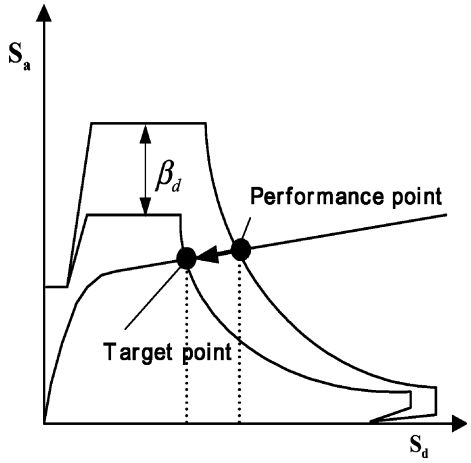

Fig. 6. Estimation of equivalent damping required to meet the target point.

required supplemental damping. The equivalent damping can be obtained as the ratio of the dissipated energy and the stored energy of the additional brace at the target point, and can also be expressed as a function of the stiffness ratio, S_r, which is the ratio of the added stiffness, k_{add}, and the initial stiffness, K_{init}. In the case of a Type-B brace system, where knee braces are placed beneath the beams, the equivalent damping can be obtained as

$$\zeta_{add} = \frac{1}{4\pi}\frac{4(\delta_t - \delta_y)Q_y}{\frac{1}{2}K_{\sec}\delta_t^2 + \frac{1}{2}}Q_y\delta_t = \frac{2}{\pi}\frac{(\mu-1)S_r}{\mu(\mu\psi + S_r)}, \tag{16}$$

where $K_{\sec} = \Psi K_{init}$, $\Psi = (\alpha\mu - \alpha + 1)/\mu$, $\mu = \delta_t/\delta_y$ is the ductility ratio, α is the post-yield stiffness ratio, $\delta_y = (\xi l_b \sigma_y L)/[(A+B)E\cos\theta]$ is the displacement at yield, E is the elastic constant, δ_t is the target displacement, and $A = \xi l_b \sin\theta$, $B = d_b\cos\theta$. From Eq. (16) the stiffness ratio of the added stiffness and the initial stiffness, S_r, can be obtained as follows:

$$S_r = \frac{K_{add}}{K_{init}} = \frac{\pi\mu^2\zeta_{add}\psi}{\{2(\mu-1) - \pi\mu\zeta_{add}\}}. \tag{17}$$

Therefore the cross-sectional area of the BRKB needed to meet the target point, A_b, can be obtained as follows using Eqs. (1) and (17):

$$A_b = \frac{\frac{2\pi^3 m}{T^2}\zeta_{add}\delta_t}{\delta_{by}\left(\frac{\delta_t}{L}(A+B) - \frac{\xi l_b \delta_{by}}{E\cos\theta}\right) - \frac{\pi(A+B)E}{2L}\zeta_{add}\cos\theta} \tag{18}$$

where T and m are the elastic period and the mass of the structure, respectively. For a multi-story structure with Type-B brace, the required additional cross-

sectional area can be obtained as follows:

$$A_b = \frac{\frac{2\pi^3}{T^2}\zeta_d \sum_j m_j \delta_{tj}}{\sigma_{by} \sum_j \gamma_j \left(\frac{\delta_{tj}}{L}(A+B) - \frac{\xi l_b \sigma_{by}}{E\cos\alpha} \right) - \frac{\pi(A+B)}{2L}\zeta_d \sum_j \gamma_j \delta_{tj} E\cos\alpha}. \tag{19}$$

From the total amount of the sectional area the size of braces to be installed in the ith story, A_{di}, is determined using a proper distribution factors, γ_i, which are determined from quantities such as inter-story drift ratios, story stiffness, etc.:

$$A_{bi} = \gamma_i A_b. \tag{20}$$

The required amount of Type-M brace can be obtained similarly to Type-B. For Type-T model the required equivalent damping ratio, stiffness ratio, and the sectional area are computed as follows:

$$\zeta_d = \frac{2}{\pi} \frac{(\delta_t - \delta_{y1})\delta_{by1} S_{r1} + (\delta_t - \delta_{y2})\sigma_{by2} S_{r2}}{\delta_t \{\psi \delta_t + (S_{r1}\delta_{y1} + S_{r2}\delta_{y2})\}} \tag{21}$$

$$S_{r1} = \frac{\pi \zeta_b \psi \delta_t^2 (A+B)}{\delta_{y1}[2\{(A+B)(\delta_t - \delta_{y1}) + A(\delta_t - \delta_{y2})\} - \pi \zeta_d \delta_t (2A+B)]} \tag{22a}$$

$$S_{r2} = \left(\frac{A}{A+B} \right) S_{r1} \tag{22b}$$

$$A_b = \frac{\frac{2\pi^3}{T^2}\zeta_d \sum_j m_j \delta_{tj}}{\sigma_{by} \sum_j \gamma_j \left(\frac{\delta_{tj}}{L}(2A+B) - \frac{2\xi l_b \sigma_{by}}{E\cos\alpha} \right) - \frac{\pi(2A+B)}{2L}\zeta_d \sum_j \gamma_j \delta_{tj} E\cos\alpha}, \tag{23}$$

where S_{r1} and S_{r2} are the stiffness ratio of the lower and upper braces to the initial stiffness of the structure. The displacements at the yield of the lower and the upper braces, δ_{y1} and δ_{y2}, respectively, are as follows:

$$\delta_{y1} = \frac{\xi l_b \sigma_{by} L}{(A+B)E\cos\theta}; \quad \delta_{y2} = \frac{\xi l_b \sigma_{by} L}{AE\cos\theta}. \tag{24}$$

The size of the brace obtained in Eqs. (19) and (20), however, is not the final one because the capacity curve increases and the effective period at the target displacement decreases with the installation of the additional brace. Therefore with the first trial value for the size of additional BRKB, new capacity curve is constructed, and the required effective damping of the system and the equivalent damping of the structure at target point are computed again. Then the next trial size of the additional brace can be computed. The trial values will converge fast after a few iterations.

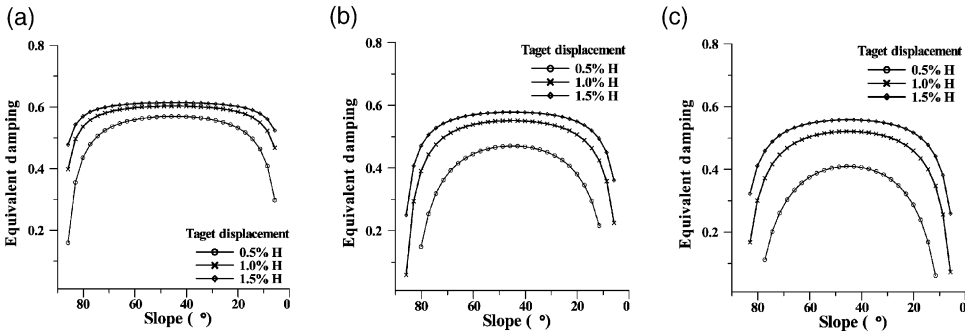

Fig. 7. Variation of equivalent damping for slope of knee brace. (a) $\sigma_{by} = 100$ MPa, (b) $\sigma_{by} = 240$ MPa; (c) $\sigma_{by} = 330$ MPa.

4. Parametric study

In this section the effect of the slope (θ), cross-sectional area (A_b), and yield stress (σ_{by}) of the knee brace on the equivalent damping and on displacement response of a structure is investigated. A single-story, one-bay structure composed of 4 m high wide flange columns (H250×250×9×14 (mm)), a 6 m wide beam (H400×200×8×13), and two buckling-restrained knee braces is analyzed for parametric study. It is assumed that all the members are connected by hinges. Nonlinear dynamic analyses are carried out using the program code DRAIN2D+ [6] with El Centro (NS) earthquake and two artificial earthquakes EQ1 and EQ2 as an input ground excitation. The generation of the artificial earthquakes will be addressed in the next section. Three types of braces with yield stress of 100, 240, and 330 MPa were used in the analysis. The cross-sectional areas used in the plotting were determined so that the maximum displacements of the structure range from 2.5% to 1.5% of the story height, and that the lateral stiffness of the structure is the same for the three yield stresses of the knee brace.

Fig. 7 plots the change in equivalent damping ratio of the structure for various slope, cross-sectional area, and yield stress of the BRKB at the moment that the structure was pushed to the maximum displacement of 2.5% of the structure height. For the model structure, the equivalent damping can be represented as the following closed form expression in reference to Fig. 4(b)

$$\zeta_{eq} = \frac{1}{4\pi}\frac{4(\delta_t - \delta_y)Q_y}{\frac{1}{2}Q_y\delta_t} = \frac{2}{\pi}\frac{(\mu - 1)}{\mu}. \tag{25}$$

By substituting $\mu = \delta_t/\delta_y$, $\delta_y = (\xi l_b \sigma_{by} L)/[(A + B)E\cos\theta]$, $A = \xi l_b \sin\theta$ and $B = d_b\cos\theta$, the above equation can be transformed to the following form:

$$\zeta_{eq} = \frac{2}{\pi}\left(1 - \frac{2l_h\sigma_{by}L}{(l_h + d_b)E\delta_t \sin 2\theta}\right). \tag{26}$$

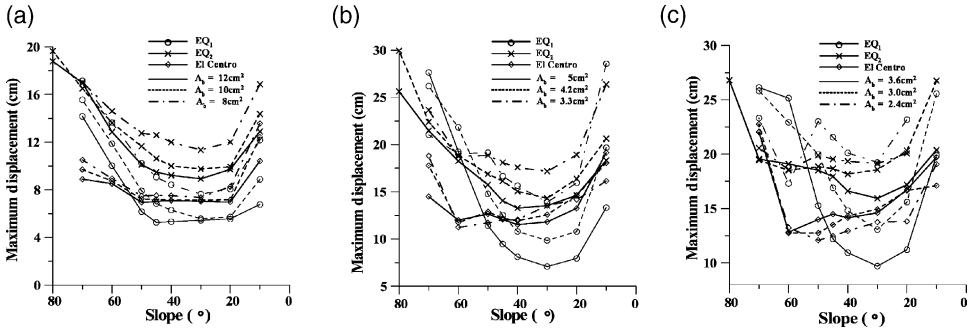

Fig. 8. Variation of maximum displacement for slope of knee brace. (a) $\sigma_{by} = 100$ MPa, (b) $\sigma_{by} = 240$ MPa; (c) $\sigma_{by} = 330$ MPa.

The definition of the variables can be found in the previous sections. The optimal slope of the knee braces that maximize the equivalent damping can be found by equating the derivative of Eq. (26) with respect to the slope to zero

$$\frac{d\zeta_{eq}}{d\theta} = -\frac{8\ l_h Q_y L}{\pi(l_h + d_b)E\delta_{sp}} \frac{\cos 2\theta}{\sin^2 2\theta} = 0, \tag{27}$$

where it can be found that the equivalent damping is maximized when the slope is 45°. It also can be observed that the optimum slope is independent of the material property of the brace. The variation of the equivalent damping for the change in design parameters can be observed by substituting specific values to Eq. (26). It can be found in the figure that the equivalent damping becomes maximum when the slope of the knee brace is 45° and that the equivalent damping decreases as the slope deviates from 45°. It also can be observed that the magnitude of equivalent damping increases as the maximum displacement increases and the yield stress of brace decreases. It is interesting to notice that as the yield stress of braces decreases the curves for equivalent damping becomes flatter for wider range of slopes.

Fig. 8 presents the maximum displacement of the structure obtained from time–history analysis using the three different earthquake records. As can be expected from the results of equivalent damping, the maximum displacement increases rapidly as the slope of the braces increases above 60° and decreases below 20°. It also can be seen that for structures with the same lateral stiffness the maximum displacement decreases as the yield stress of the brace decreases. In most cases the maximum displacements are minimized when the braces are placed with the slope within 20°–60°. No particular value can be found for the optimum brace slope.

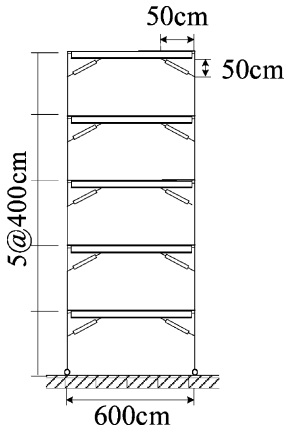

Fig. 9. Model structure for analysis. (a) Design and response spectra. (b) Time–history of the artificial earthquake record.

5. Application of the proposed procedure

5.1. Design of the model structure

The knee braces in the one-bay five-story model structure shown in Fig. 9 were designed first in accordance with the current Korean seismic design provision [3]. The design parameters used in the evaluation of the base shear have the following values: zone factor A = 0.11, soil factor S = 1.2, importance factor I = 1.0, and the response modification factor R = 3.5 (braced frame). The lateral load was assigned only to the knee braces. The hinge-connected beams and columns were designed to resist only the gravity load. The mass of each story is 100 kN, and the sizes of the designed structural members are given in Table 1.

Pushover analysis was carried out with the lateral seismic load proportional to the fundamental mode shape. Table 2 presents the ratios of story stiffness, story shear, and the inter-story drifts obtained from the pushover curve which is idealized as bi-linear lines. The ratios will be used later as coefficients for distributing the total cross-sectional area of brace, required to meet the target performance point, to each story.

5.2. Performance evaluation of the model structure

The seismic performance of the model structure was evaluated using nonlinear static and dynamic analyses. The design spectrum presented in Fig. 10(a) with the seismic coefficients $C_a = 0.44$ and $C_v = 0.74$, as suggested in the 'Performance-based seismic design guideline of Korea' [7] for earthquake with return period of 2400 years, was used for the CSM. To validate the accuracy of the seismic design procedure, time–history of earthquake excitation, shown in Fig. 10(b), was generated based on the design spectrum [8], and nonlinear dynamic time history analysis

Table 1
Member size of the model structure

Story	Columns	Beams	Sectional area of knee brace (cm^2)
5	H250×250×9×14	H400×200×8×13	2.14
4	H250×250× 9×14	H400×200×8×13	3.85
3	H300×300×10×15	H400×200×8×13	5.13
2	H300×300×10×15	H400×200×8×13	5.99
1	H300×300×10×15	H400×200×8×13	6.41

was performed using the artificial earthquake record. The response spectrum constructed using the time history record is also plotted in Fig. 10(a).

Table 3 presents the maximum displacements obtained from both static and dynamic analyses, which shows that the difference between the two results is not significant. If the target displacements are set to be 20 cm and 25 cm, the performance point exceeds the targets, and the size of knee braces needs to be increased to meet the target displacement. The proper size of additional braces can be estimated using the equivalent damping ratio required to be supplemented to meet the target. The required equivalent damping to meet the target displacements obtained following the procedure presented above is also shown in Table 3.

5.3. *Story-wise distribution of knee braces*

The required cross-sectional area of knee braces in each story to meet the given target displacement is obtained using Eq. (20) and proper distribution factors. In this study the size of knee braces in each story is determined based on the following four story-wise distribution types:

- Case A: The same size of knee brace is used in each story;
- Case B: The size of knee brace is proportional to the story-stiffness;
- Case C: The size of knee brace is proportional to the story-shear;
- Case D: The size of knee brace is proportional to the inter-story drift obtained from pushover analysis.

Table 2
Story-wise distribution factors γ for the knee brace

Story	Story stiffness ratio	Story shear ratio	Inter-story drift ratio
5	0.56	0.39	0.23
4	0.89	0.61	0.34
3	0.97	0.78	0.44
2	0.98	0.91	0.57
1	1.00	1.00	1.00

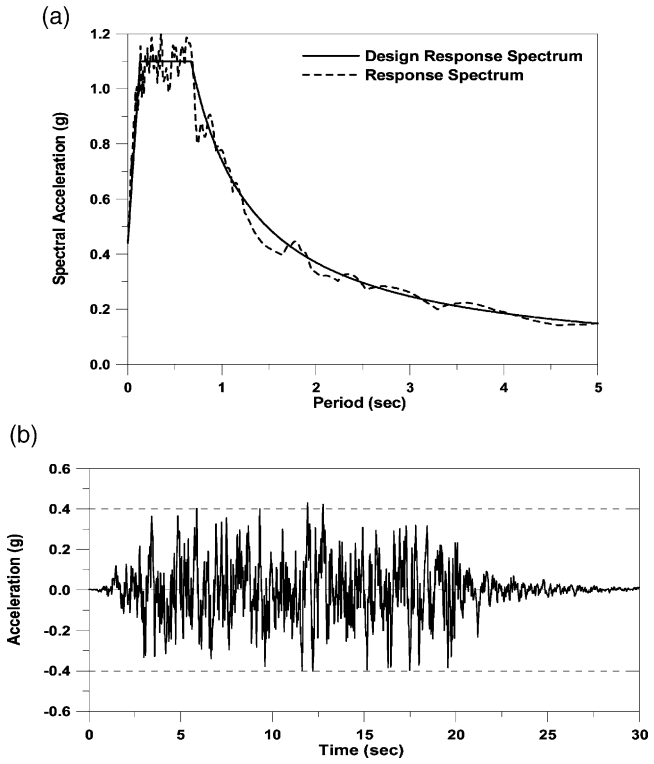

Fig. 10. Seismic load used in the analysis. (a) Case A, (b) case B, (c) case C (d) case D.

The story-wise distribution factors γ_i for Case B to Case D are shown in Table 2. For Case A distribution, the same distribution factor is used in each story. Two types of yield stress of braces, $\sigma_{by} = 100$ MPa and 240 MPa, are used in the design. Table 4 presents the cross-sectional area of the knee braces designed to reduce the maximum displacement to the target displacement, which shows that the total cross-sectional area of the knee brace used in the retrofit is lowest in Case D.

Table 3
Maximum displacement and required equivalent damping

Target displacement (cm)	CSM	Time history analysis (cm)	Required damping (β_d)
20	30.2	32.2	0.310
25			0.108

Table 4
Story-wise distribution of knee brace

Distribution type	Story	Sectional area of knee brace (cm^2)	
		$u_m = 20$ cm	$u_m = 25$ cm
Case A	5	8.35	3.68
	4	10.06	5.39
	3	11.34	6.67
	2	12.20	7.52
	1	12.62	7.95
	Total	**54.56**	**31.21**
Case B	5	9.37	3.96
	4	11.31	5.73
	3	12.44	6.97
	2	12.62	7.66
	1	10.81	7.52
	Total	**56.56**	**31.84**
Case C	5	4.94	2.85
	4	8.29	4.96
	3	10.80	6.55
	2	12.61	7.64
	1	13.69	8.24
	Total	**50.36**	**30.24**
Case D	5	4.23	2.67
	4	6.94	4.63
	3	9.14	6.14
	2	11.18	7.30
	1	15.52	8.71
	Total	**47.01**	**29.45**

5.4. Numerical results

The maximum displacements in each story of the model structure with the BRKB designed following the above-mentioned procedure were obtained from time–history analysis and are shown in Fig. 11 and Table 5. It can be observed in the figure that in most cases the maximum roof-displacements are close to the target displacement when knee braces with yield stress of 100 MPa are used, while there are noticeable difference when knee braces with yield stress of 240 MPa are used. It also can be seen that the deformation shape of the model structure differs significantly depending on the distribution pattern of the brace. Especially the Case D distribution pattern for brace results in the maximum story displacement shape close to the linear line. From a standpoint of damage distribution and efficiency in material use, the linear deformation shape seems to be the most desirable. Table 5 shows that the story-wise distributions of the brace following the Case A and D distribution patterns provide the most accurate results with least amount of braces. In Case B and C larger amount of braces are required to meet the target, even though the displacement results are less accurate than the other cases. Generally

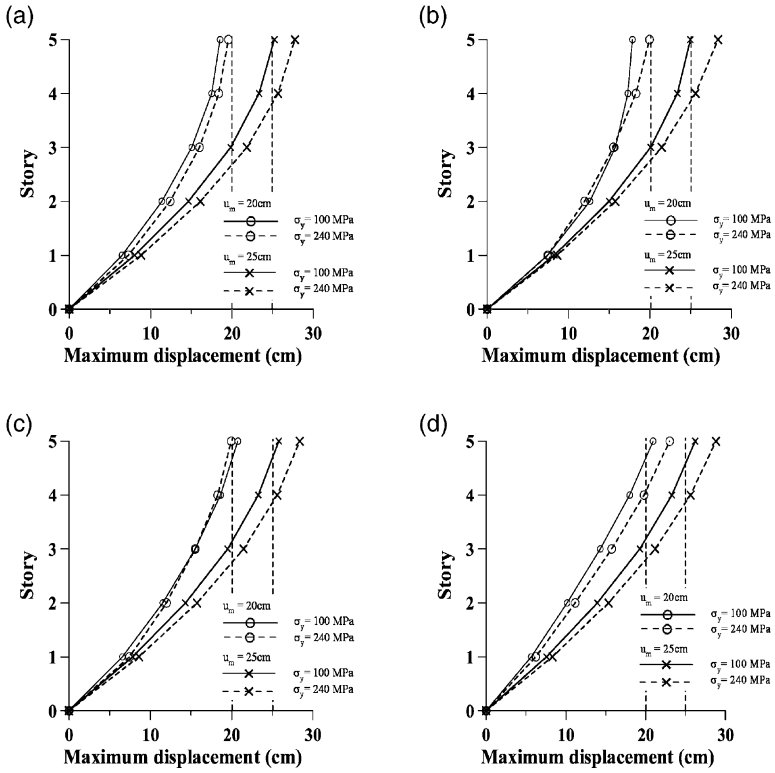

Fig. 11. Maximum displacement of the model structure for different story-wise distribution of knee brace. (a) $u_m = 25$ cm, (b) $u_m = 20$ cm.

the difference between the target displacement and the maximum displacement is larger when the braces with $\sigma_{by} = 240$ MPa is used.

Fig. 12 plots the ductility demands of the braces in each story. The BRKB with yield stress of 100 MPa are used in the analysis. It can be observed that when the target displacement u_m is set to be 25 cm at the top story, all braces yield; whereas the braces in the fifth story in Case A, B and C remain elastic when $u_m = 20$ cm. This explains the over-controlled maximum roof displacements in Case A and B as shown in Fig. 11. It can be observed in Fig. 12 that the ductility demands in braces are higher in lower stories, as expected, and are more uniformly distributed in Case D, which is more desirable in that all braces can display their full capacity at ultimate state.

Fig. 13 illustrates the seismic input energy (E_I), viscous damping energy (E_D), and the plastic hysteretic energy dissipated by knee braces (E_P). For the target displacement of 25 cm, the energy quantities are similar in each distribution case. However for the target displacement of 20 cm, the plastic energy E_P is smaller in

Table 5
Maximum story displacements of the model structure

Distribution type	Story	Maximum displacement (cm)	
		$u_m = 20$ cm	$u_m = 25$ cm
Case A	5	**18.54**	**25.21**
	4	17.51	23.33
	3	15.05	19.85
	2	11.38	14.66
	1	6.50	8.04
	Target/Max	**0.93**	**1.01**
Case B	5	**17.85**	**24.95**
	4	17.29	23.36
	3	15.74	20.09
	2	12.61	14.98
	1	7.42	8.26
	Target/Max	**0.89**	**1.00**
Case C	5	**20.75**	**25.79**
	4	18.63	23.27
	3	15.51	19.50
	2	11.52	14.30
	1	6.57	7.82
	Target/Max	**1.04**	**1.03**
Case D	5	**20.93**	**26.20**
	4	18.00	23.30
	3	14.31	19.26
	2	10.15	13.95
	1	5.66	7.56
	Target/Max	**1.05**	**1.05**

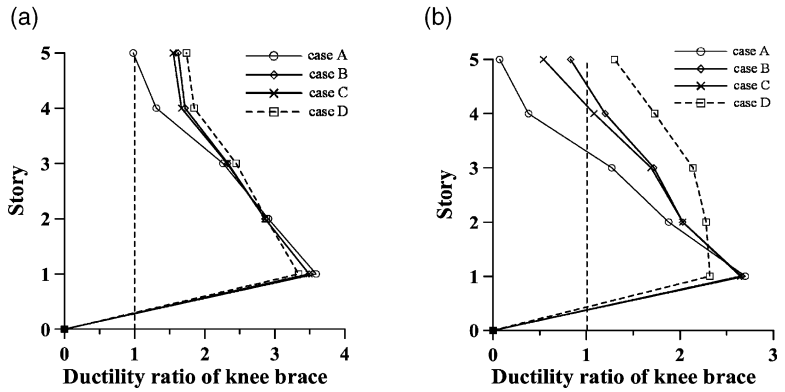

Fig. 12. Ductility demand of knee brace in each story. (a) $u_m = 25$ cm, (b) $u_m = 20$ cm.

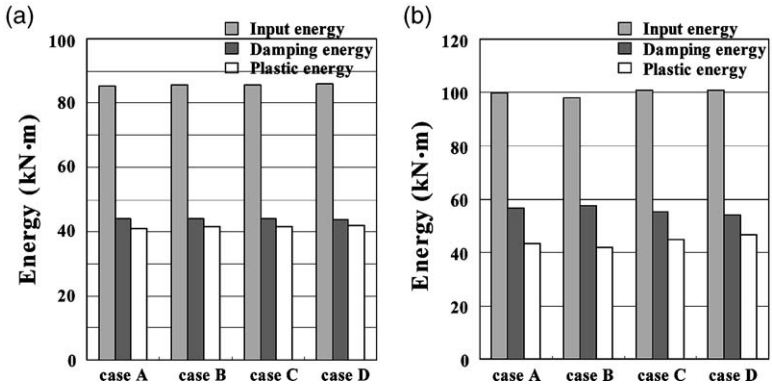

Fig. 13. Seismic energy in the model structure. (a) $u_m = 25$ cm, (b) $u_m = 20$ cm.

Case A and Case B compared to other cases because the braces in upper stories do not yield, as can be observed in Fig. 12(b).

Fig. 14 plots the story-wise distribution of energy dissipated by the braces, where it can be noticed that energy dissipation is concentrated in the lower stories. Among the brace distribution patterns, the Case D distribution results in lower energy dissipation in the lower stories and higher dissipation in the upper stories compared to the other distribution cases, which is more desirable. This coincides with the findings in Fig. 13.

Fig. 15 plots the maximum bending moments induced in beams and columns divided by the yield moment of each member. In all cases the bending moment transferred to beams turned out to be insignificant for the given example. However, the maximum moment ratio of columns can be as high as 50% especially when the target displacement is 20 cm. Therefore in this case the columns need to

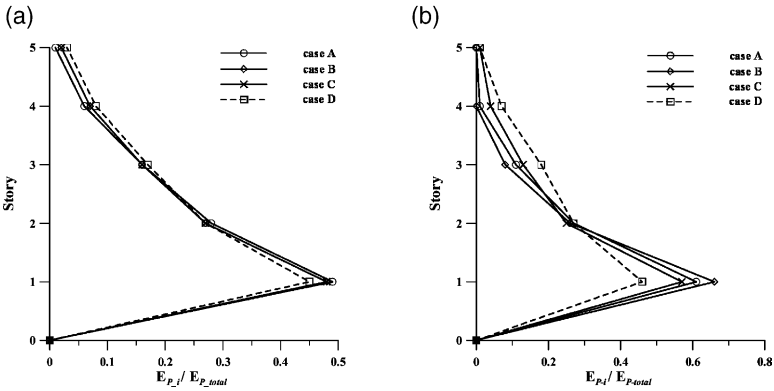

Fig. 14. Energy dissipated by knee brace in each story. (a) case A, (b) case B, (c) case C, (d) case D.

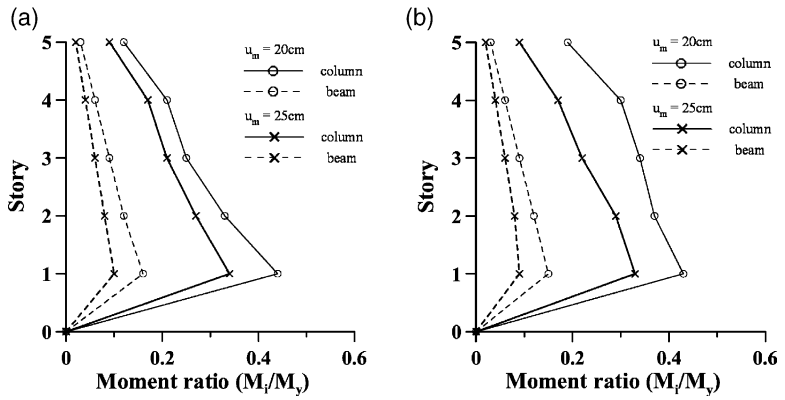

Fig. 15. Bending moment in structural members connected to the knee braces.

be designed conservatively considering the transfer of lateral load from knee-braces.

6. Conclusions

This study presents a seismic design procedure for a framed structure with buckling-restrained knee braces. The hinge-connected beams and columns were designed mainly to resist gravity load, and the knee braces were designed to resist the lateral seismic load. In the preliminary design stage, the braces were designed for the base shear computed in accordance with the current Korean seismic design code. Then the seismic performance of the structure was evaluated using the CSM. Two levels of target displacements smaller than the performance point were specified, and the cross-sectional area of the knee braces required to meet the target was computed.

The time–history analysis of a five-story model structure designed following the proposed procedure showed that, although depending on how the braces were distributed along the stories, the structures retrofitted by the proposed method generally satisfied the given target performance point. Also it was observed that the main structural members such as beams and columns remained elastic, whereas all the knee-braces deformed inelastically dissipating all the vibration energy induced by the earthquake. This corresponds with the intended design philosophy that the damage due to inelastic deformation is limited to the lateral load resisting elements.

Acknowledgements

This research is funded by the Korea Science and Engineering Foundation under Grant No. R01-2002-000-00025-0. This financial support is gratefully acknowledged.

References

[1] Huang YH, Wada A, Sugihara H, Narikawa M, Takeuchi T, Iwata M, Seismic performance of moment resistant steel frame with hysteretic damper. Proceedings of the Third International Conference STESSA, Montreal, Canada, 2000.
[2] Suita K, Inoue K, Takeuchi I, Uno N, Mechanical Behavior of Bolted Beam-to-Column Connections with Hysteretic Damper, The 3rd Japan-Korea_Taiwan Joint Seminar on Earthquake Engineering for Building Structures, Taipei, Taiwan, 2001.
[3] Architectural Institute of Korea, Regulations for building design loads, 2000.
[4] ATC, Seismic Evaluation and Retrofit of Concrete Buildings, ATC-40 Report, Applied Technology Council, Redwood City, CA, 1996.
[5] FEMA. NEHRP Guidelines for the Seismic Rehabilitation of Buildings, FEMA273, October. Washington, DC: Federal Emergency Management Agency; 1997.
[6] Tsai KC, Li JW, DRAIN2D+, A general purpose computer program for static and dynamic analyses of inelastic 2D structures supplemented with a graphic processor, Report No.CEER/R86-07, National Taiwan University, Taipei, Taiwan, 1997.
[7] Korea Institute of Earthquake Engineering, Report on performance-based seismic design provision, 1997.
[8] Vanmarcke EH, Gasparini DA. A Program for Artificial Motion Generation, User's Manual and Documentation. Dept. of Civil Engineering, Massachusetts Institute of Technology; 1976.